Vol. 25, No. 16

Identification of Splicing Silencers and Enhancers in Sense *Alu*s: a Role for Pseudoacceptors in Splice Site Repression†

Haixin Lei[1,2] and Igor Vořechovský[1]*

*University of Southampton School of Medicine, Division of Human Genetics, Southampton SO16 6YD,
United Kingdom,[1] and Karolinska Institute at NOVUM, Department of Biosciences,
S-141 57 Huddinge, Sweden[2]*

Auxiliary splicing signals in introns play an important role in splice site selection, but these elements are poorly understood. We show that a subset of serine/arginine (SR)-rich proteins activate a cryptic 3′ splice site in a sense *Alu* repeat located in intron 4 of the human *LST1* gene. Utilization of this cryptic splice site is controlled by juxtaposed *Alu*-derived splicing silencers and enhancers between closely linked short tandem repeats TNFd and TNFe. Systematic mutagenesis of these elements showed that AG dinucleotides that were not preceded by purine residues were critical for repressing exon inclusion of a chimeric splicing reporter. Since the splice acceptor-like sequences are present in excess in exonic splicing silencers, these signals may contribute to inhibition of a large number of pseudosites in primate genomes.

Most eukaryotic genes contain introns that are removed from pre-mRNAs by splicing. The removal of introns occurs in two sequential transesterification reactions that are catalyzed by a large ribonucleoprotein (RNP) complex termed the spliceosome (10). The formation of the spliceosome involves the stepwise assembly of snRNPs (U1, U2, U4/U6, and U5) and a large number of non-snRNP proteins on a pre-mRNA. The spliceosome assembly is characterized by multiple and relatively weak interactions that require conserved *cis*-acting elements in the pre-mRNA: the 5′ splice site (5′ ss), 3′ ss, polypyrimidine tract (PPT), and the branchpoint sequence (BPS). In higher eukaryotes, these consensus signals are necessary but often insufficient to define exon-intron boundaries and efficient splicing requires auxiliary *cis* elements that activate or repress splicing, known as exonic splicing enhancers (ESEs) and intronic splicing enhancers or exonic splicing silencers (ESSs) and intronic splicing silencers. These signals allow the genuine splice sites to be correctly recognized among a vast excess of pseudosites that have similar sequences but outnumber authentic splice sites by an order of magnitude (10, 22, 60). The auxiliary signals have been identified through mutations that alter splicing, through computational comparisons, and through selection of sequences that activate or repress splicing or bind to splicing regulatory proteins (16, 23, 61, 65, 68). Exonic sequences, which often regulate both constitutive and alternative splicing through binding of serine/arginine-rich (SR) proteins (6, 27) and are important for exon definition (3), have been studied more extensively than auxiliary signals in introns. In particular, repression of pseudosites by intronic splicing silencers has been poorly understood (22, 60).

Introns contain several classes of repetitive elements that

have been shown to influence pre-mRNA splicing. Short tandem repeats (STRs), or 1- to 6-bp iterative motifs called microsatellites, were reported to affect pre-mRNA splicing of at least four human genes if located close to the 3′ or 5′ ss (1, 25, 28, 33, 51). *Alu* repeats, the largest family of mobile elements in the human genome (2), can be exonized by a single or two point mutations if they are in the antisense orientation (44, 47, 58) and provide a source of ready-to-use segments with a coding potential (45, 46). In yeast (*Saccharomyces cerevisiae*), extensive self-complementarity in intronic sequences has been shown to promote exon definition (32), suggesting that repetitive sequences could have a more general and underappreciated role in gene expression.

The *LST1* gene encodes a leukocyte-specific transcript with a predominant expression in monocytes and dendritic cells (31, 52). *LST1* generates at least 14 alternatively spliced variants (designated *LST1/A* to *LST1/N*) that encode transmembrane as well as soluble molecules (53). The predicted polypeptides vary with regard to the presence of the N- and C-terminal sequences and have been shown to differentially stimulate lymphocyte proliferation, suggesting that *LST1* plays a role in the immune system (19, 53). Overexpression of *LST1* isoforms that contain the transmembrane domain induced the formation of long filopodia and microspikes at the cell surface (52), but the exact function of the gene is not understood. *LST1* is located in the major histocompatibility complex class III region centromeric of the gene for tumor necrosis factor alpha (TNF-α) in an area predicted to encode genes that have a role in mRNA processing (42). The *LST1* gene contains well-known STRs that were termed TNFd and TNFe (63) and mapped close to the alternative 3′ ss of intron 4 (31).

Here, we have investigated a role of TNFd and surrounding sequences in alternative splicing of *LST1*. We show that an SR-induced activation of a cryptic splice acceptor located in a sense *Alu* repeat between TNFd and TNFe is influenced by a downstream *Alu*-derived segment that contains juxtaposed splicing silencers. Systematic mutagenesis of these elements in a heterologous context revealed that AG dinucleotides that

---

* Corresponding author. Mailing address: University of Southampton School of Medicine, Division of Human Genetics, Duthie Building, MP808, Southampton SO16 6YD, United Kingdom. Phone: 44 2380 796425. Fax: 44 2380 794264. E-mail: igvo@soton.ac.uk.

were not preceded by purine residues were critical for the inclusion of *Alu*-derived sequences in mature transcripts. Since these acceptor-like sequences are overrepresented in ESSs, we propose that they play an important role in suppressing a large number of pseudosplice sites in the primate genomes.

MATERIALS AND METHODS

Minigene constructs and site-directed mutagenesis. The *LST1* minigene was cloned into pCR3.1 (Invitrogen) with primers 1F (5′-AACTGTTGGAGAGGG AATCTGAGA) and 1R (5′-ATTCAAAGGTCAAAAAGCCACATA) (Fig. 1A). This minigene contains TNFd allele d3 characterized by a (AG)$_{14}$GG(AG)$_9$ repeat. The allelic structure of TNFd and TNFe is shown in Table S1 in the supplemental material. The *XPC* construct, which was derived from the human gene deficient in *x*eroderma *p*igmentosum (group *C*) and contains exons 3 through 5, was cloned into EcoRV/XbaI sites of pCR3.1 with primers 5′-CGT AGATATCATCTTCCTTCCTGTGGTCTTTACAC and 5′-TAGCTCTAGAC TTCCCCATCATTCCTTGCCCTTAC. The *t*runcated *XPC* construct *XPC-T* was created with mutagenic primers xpc-din3-f (AAGAAGGCTGAGACTGTC TGGGTTGTGTGG) and xpc-din3-r (CAGACAGTCTCAGCCTTCTTTGGT AACTTG). The *TH* minigene, which contains exons 11 through 13 of the human gene for *t*yrosine *h*ydroxylase, was cloned into EcoRI/XbaI sites of the same expression vector using primers 5′-GACTGAATTCGGCTGCCTCTCCCCAT CCTTC and 5′-GATCTCTAGAAGCAGCCTAGCCCACCTGAGC. The chimeric *XPC* and *TH* minigenes were prepared by inserting *Alu*-derived *LST1* segments 24 nucleotides (nt) downstream of the 3′ ss of *XPC* intron 3 and *TH* intron 11. An ASF/SF2 cDNA clone containing a 21-nt deletion (CGGCGGGG GGTGGAGGTGGCGG) that removes a heptaglycine stretch between RNA recognition motif 1 (RRM1) and RRM2 was obtained by amplifying cDNAs prepared from HeLa cells with primers A1 (ATCCTCGAGATGTCGGGAGG TGGTGTGATT)and A2 (ATCACGCGTCAACATGGGTTCTACAAAAAG).

Mutated clones were obtained by two-step overlap extension PCR (30). A→G mutations of the predicted branchpoint (BP) adenines of *XPC* exon 4 and *TH* exon 12 were introduced with mutagenic primers 5′-ACTATTACTG**G**TTTTT AAAAA and 5′-CTCTGGGCTG**G**TGCTGCCCGGC, respectively (mutation is in bold). BPs of both exons were mapped previously in case reports of disease-causing BPS mutations that produced splicing defects (34, 39) and through our own investigation (I.V. et al., in preparation). A 48-bp polylinker (PL) sequence (ACTAGTGCGGCCGCCTGC**A**GGTCGACCATATGGGAGAGCTCCCAA CGC) was used for TNFd replacements to generate constructs TNFd-PL (Fig. 1B). Clone TNFd-(AG)$_0$-A>PL was prepared by replacing segment A (Fig. 1A) with the first 38 bp of PL, except for an A-to-T transversion (in bold in the PL sequence) to destroy a potential 3′ AG. All wild-type and mutated reporter constructs were sequenced using the automated ABI377 sequencer as described previously (64) to confirm intended changes and exclude clones with undesired mutations. ASF/SF2 constructs described previously (12) were a generous gift of G. Screaton (University of Oxford) and J. Cáceres (University of Edinburgh). Wild-type and mutated ASF/SF2 constructs were validated by sequencing.

Cell cultures and transfection. Transient transfections were performed in six-well (growth area, 9.4 cm^2) plates with FuGENE 6 (Roche) as described previously (41). The plating density was 1.5×10^5. When reaching ~50% confluence, the medium was changed 2 h before adding DNA mixture, which was prepared by combining 3 μl of FuGENE and 50 μl of serum-free medium, followed by addition of plasmid DNA (1 μg, except for cotransfection experiments [see figure legends] purified with the Wizard Plus SV Minipreps (Promega). The DNA mixture was incubated for 20 min at room temperature prior to transfections. Cells were harvested for RNA extraction 48 h posttransfection. The amounts of plasmids expressing SR proteins are shown in the figure legends.

RNA extraction and detection of RNA products. Total RNA was extracted using Tri reagent (Sigma) according to the manufacturer's recommendation and measured on a spectrophotometer. Five hundred nanograms of RNA was reverse transcribed with primer PL2 (CCGACTAGTCGCCCAAAT) and Moloney murine leukemia virus reverse transcriptase (RT; Promega) at 42°C. RT was inactivated for 5 min at 95°C. RT-PCR was performed with vector primers PL1 (ACTCACTATAGGGAGACC) and PL2 and validated by a combination of vector and cDNA primers 2F (TCTGTCCGCCTGCCTGTGTTG) and 2R (G GATCCTCCTTGGTGCCTCTC; Fig. 1A). PCR products were separated on polyacrylamide (Fig. 1C) or agarose gels. RNA products were confirmed by sequencing as described previously (64). The relative ratios of RNA products were measured with FluorImager 595 using FluorQuant and Phoretix software packages (Nonlinear Dynamics Inc.) for at least two transfections in duplicate as described previously (41).

RESULTS

SR-mediated activation of a cryptic 3′ ss in *LST1* intron 4. TNFd and TNFe are highly polymorphic STRs located upstream of the alternative 3′ ss of *LST1* intron 4 (Fig. 1A). To determine their organization, we sequenced both STRs in cell lines homozygous in the major histocompatibility complex (see Table S1 in the supplemental material). The structure of TNFd was (AG)$_{12–16}$GG(AG)$_{9–11}$ on the analyzed haplotypes, whereas TNFe was a simple (AG)$_{7–9}$ repeat. To test if TNFd, which is located ~70 bp upstream of the proximal splice acceptor site (Fig. 1A; and see Fig. S1 in the supplemental material), can influence alternative 3′ ss selection, we transfected minigene constructs that contained TNFd allele d3 [(AG)$_{14}$GG(AG)$_9$, minigene TNFd-WT], a TNFd deletion [TNFd-(AG)$_0$], and a PL sequence replacing TNFd (minigene TNFd-PL) into 293T cells. Examination of the minigene splicing pattern showed that splicing reporters lacking TNFd generated RNA products identical to those observed for the wild-type minigene (data not shown), suggesting that TNFd does not influence splicing.

To test if factors known to affect RNA processing influence selection of alternative 3′ ss, we cotransfected the splicing reporters with a panel of plasmids expressing SR proteins. Coexpression of TNFd-(AG)$_0$ and TNFd-PL, but not the wild-type construct, with ASF/SF2, SRp40, SRp55, SRp75, and, to a minor extent, 9G8 and SC35 in both 293T (Fig. 1B) and HeLa (data not shown) cells activated an upstream cryptic 3′ ss located between TNFe and TNFd. The resulting isoform was termed *LST1/n* (Fig. 1A, B). The *LST1/n* expression increased with increasing amounts of plasmids expressing SRp40 (Fig. 1C) and ASF/SF2 (data not shown) cotransfected with TNFd-(AG)$_0$ or TNFd-PL constructs. In addition, we observed upregulation of isoform *LST1/C* described previously (53) and downregulation of a novel isoform designated *LST1/O*, consistent with promotion of proximal splicing by a subset of SR proteins (Fig. 1A to C), as described first for ASF/SF2 (40).

Since most SR proteins that produced significant amounts of *LST1/n* had two RRMs (ASF/SF2, SRp40, SRp55, SRp75) (27) and those lacking the second RRM (SC35, 9G8) generated little *LST1/n* (Fig. 1B), we tested the importance of their modular domains. We cotransfected the TNFd-(AG)$_0$ construct with the wild-type ASF/SF2 and ASF/SF2 lacking RRM1, RRM2, the C-terminal RS domain (13), and a heptaglycine tract between RRM1 and RRM2 (see Materials and Methods). Deletion of either RRM1 or RRM2 eliminated *LST1/n* (Fig. 1D). In contrast, deletion of the RS domain and the intervening heptaglycine only reduced the *LST1/n* yield, suggesting that the SR-induced activation of cryptic 3′ ss depends on binding of SR proteins to the pre-mRNA and only partially on contacts made by the RS domain.

Identification of splicing silencers in sense *Alu* sequences. Interestingly, a search for sequences homologous to the region between TNFe and TNFd showed that the SR-induced cryptic 3′ ss was located in the free left *Alu* monomer (FLAM) (Fig. 2A; see also Fig. S1 in the supplemental material). *Alu*s are dimeric ~300-nt repeats that probably originated from a fusion between the left and right *Alu* monomers (35). *Alu*s in antisense orientation are amenable to exonization as they contain a strong PPT and many potential 3′ and 5′ ss, whereas exoniza-
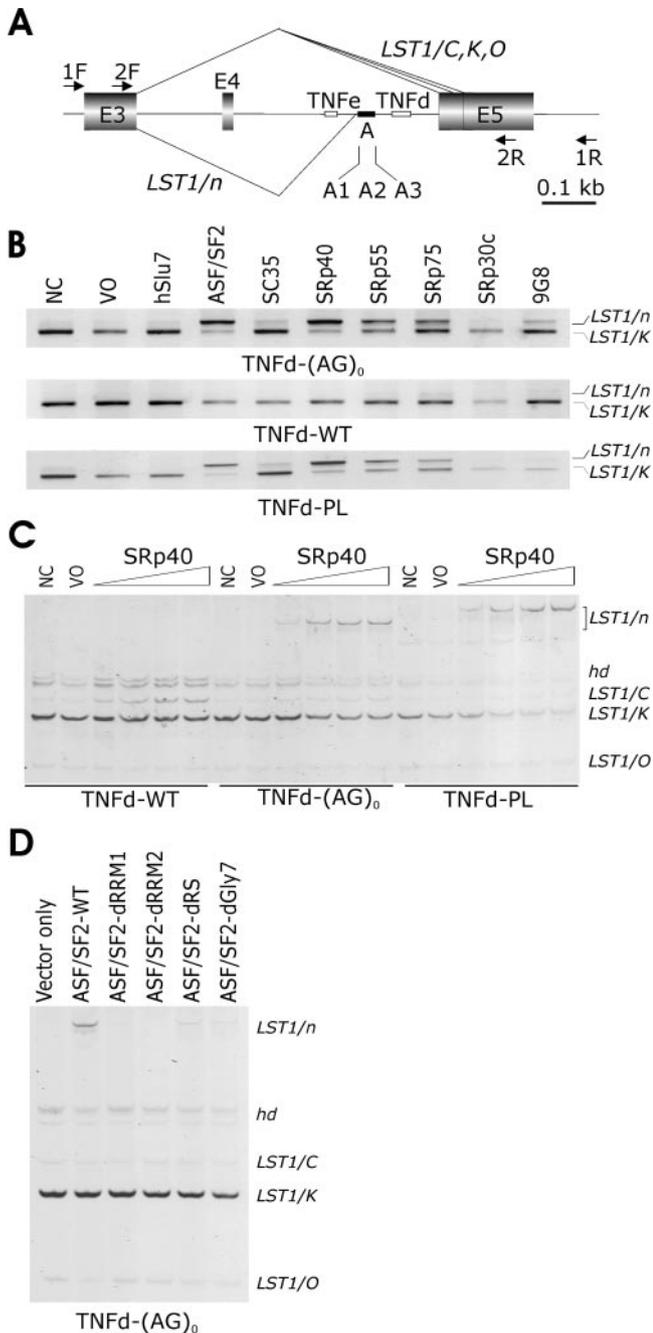
FIG. 1. SR-dependent activation of a cryptic 3′ splice site in *LST1*. (A) Schematic representation of the *LST1* minigene (to scale; scale units are kilobases). Exons are shown as shadowed boxes; introns are shown as lines. TNFe and TNFd are indicated by small open boxes; segment A is denoted by a closed rectangle. Arrows indicate primers. For a full genomic sequence of this region, see Fig. S1 in the supplemental material. Naturally occurring *LST1* isoforms arising by alternative 3′ ss and designated *LST1/C*, *LST1/K* (53), and *LST1/O* (this study) are shown above the minigene, whereas cryptic 3′ ss activation generating *LST1/n* is shown below. The location of the alternative 3′ ss of intron 4 was as described in reference 53 (and see Fig. S1 in the supplemental material). (B) Cryptic 3′ ss activation in cells overexpressing SR proteins in constructs lacking TNFd. *LST1* reporters are shown below each panel, and *LST1* RNA products are shown to the right. *LST1/K* is a predominant isoform in peripheral blood mononuclear cells generated by alternative 3′ ss of intron 4 (53). WT, wild-type; NC and VO; no-cotransfection and vector-only controls, respec-

tively. No-template controls are not shown. (C) SR-dependent upregulation of *LST1/n* and *LST1/C*. We used 0.5 μg of each reporter plasmid together with 0.1, 0.5, 1.0, and 2.0 μg of plasmids expressing SRp40. Hd, heteroduplexes. (D) Binding of ASF/SF2 to the pre-mRNA is essential for the *LST1/n* formation. d, deletion of ASF/SF2 domains RRM1, RRM2, and RS or a heptaglycine repeat (Gly7). *LST1* isoforms described above are shown on the right side.

tion of sense *Alu*s is rare (44, 57, 58). The presence of the cryptic 3′ ss in the sense *Alu* element (Fig. 2A) thus provided an opportunity to examine *Alu*-derived sequences that repress splicing.

To map *cis*-elements important for the *LST1/n* formation, we constructed a splicing reporter lacking a 38-bp segment (termed A) located between the cryptic 3′ ss and TNFd (Fig. 1A; see also Fig. S1 in the supplemental material). Interestingly, transfection of mutated constructs and sequencing of the resulting RNAs showed that this deletion activated the same cryptic 3′ ss in the absence of transiently expressed SR proteins (Fig. 2B). Replacement of this segment with a vector sequence of identical length had the same effect (Fig. 2B). Further mapping of segment A, which was subdivided into three subregions termed A1 to A3 (Fig. 1A and 2A), showed that deletion of A2 and A3 promoted cryptic splicing, whereas deletion of A1 did not (Fig. 2B), suggesting that A3 and A2 contain splicing silencers important for the *LST/n* repression.

To test how the silencers affect splicing in a heterologous context, we individually inserted A1-to-A3 subregions in both the sense and antisense orientations into the central exon of a minigene carrying exons 3 through 5 of the *XPC* gene. Intron 3 of the wild-type *XPC* minigene has a weak 3′ ss and generates an excess of exon inclusion over exon skipping, thus providing a suitable system for testing putative splicing repressors (Fig. 2C). Insertion of A2 or A3 in the sense orientation resulted in almost full exon skipping, whereas insertion of A1 had only a minor effect. In the antisense orientation, A1 and A2 constructs produced exon inclusion levels similar to those of the wild-type *XPC*, whereas insertion of A3 moderately decreased exon inclusion. Similar levels of exon skipping were produced by a *t*runcated construct (termed *XPC-T*), in which *XPC* intron 3 was shortened from ~2.1 kb to ~450 bp to facilitate mutagenesis (Fig. 2C, lower panel). In addition to *XPC*, the insertion of A3 in the sense orientation into a minigene carrying exons 11 through 13 of the human *TH* gene, which produced a mixture of exon inclusion and exon skipping in the wild type (see further below), also led to exon repression (data not shown). Together, these results suggested that A2 and A3 contained splicing silencers derived from sense *Alu*s.

Importance of AG dinucleotides for A3-mediated exon repression. To determine which A3 residues are critical for splicing, we systematically mutated each A3 position in minigene *XPC-T-A3F* to the remaining nucleotides. This *XPC-T* construct contained a 12-nt segment A3 that was inserted in the sense orientation in the central *XPC* exon. Transfection of mutated constructs into 293T cells and examination of exon inclusion showed that, unlike any other A3 dinucleotides, each single substitution of A_9G_{10} dramatically reduced exon skipping (Fig. 3A) as compared to the wild-type *XPC-T-A3F*. Similarly, mutations of A_4G_5 to cytosines significantly enhanced
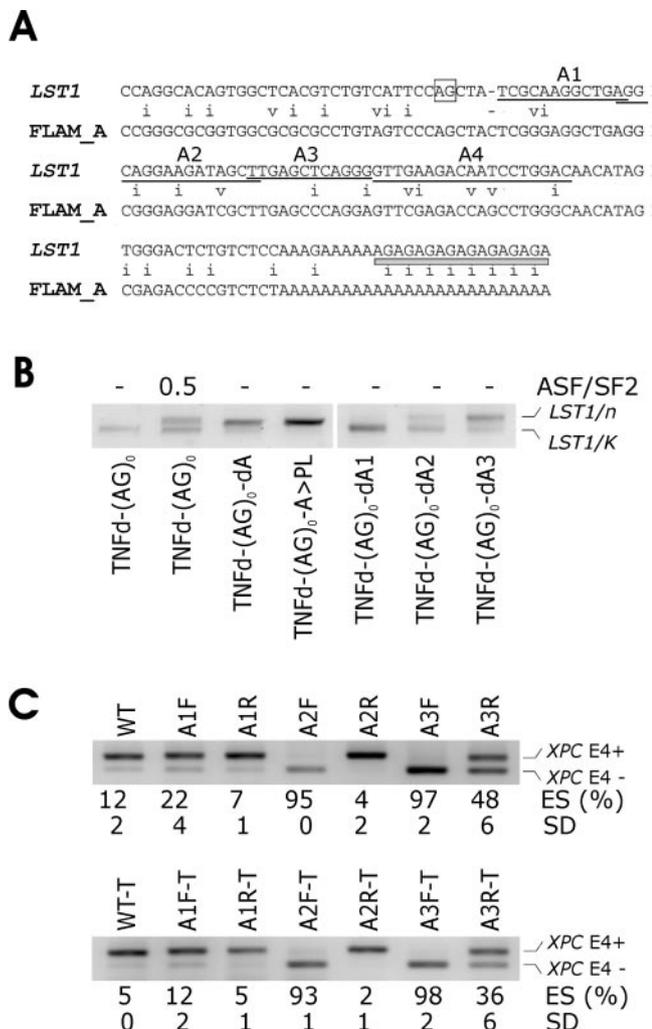
FIG. 2. Identification of *Alu*-derived splicing signals that inhibit *LST1/n*. (A) Cryptic 3′ ss and segment A sequences are derived from *Alu* repeats. Sequence alignment was generated by the RepeatMasker (http://www.repeatmasker.org/cgi-bin/WEBRepeatMasker). The cryptic 3′ ss (position 33/34 in the *Alu* consensus sequence) (2, 37) is boxed. Deleted segments A1 (positions 40 to 51 in the *Alu* consensus), A2 (positions 51 to 66), A3 (positions 66 to 77), and A4 (positions 78 to 96) are underlined. The telomeric end of TNFd is shown as a gray bar. Mismatches are indicated by the letter i (transition) or v (transversion). (B) Activation of cryptic 3′ ss upon removal of segment A3 or A2. The amount of plasmid expressing ASF/SF2 is in micrograms. Mutated constructs (bottom) are described in the text. d, deletion; >, replacement. PL refers to a polylinker sequence. Expression of *LST1/C* and *LST1/O* was negligible and is not shown. Reporter constructs containing the TNFd repeat that lacked segment A were not obtained because of a detection bias against RNA isoforms with this STR (see Fig. 1B and Discussion). (C) A3 and A2 in the sense orientation promote skipping of *XPC* exon 4. (Upper panel) Mutated minigenes transfected into 293T cells are shown at the top. F and R, *f*orward (sense) and *r*everse (antisense) orientation, respectively. ES, exon skipping as a ratio of transcripts lacking exon 4 (E4−) to the sum of E4− and E4+ transcripts. SD, standard deviation as calculated from two transfection experiments. (Lower panel) ES following transfection of the truncated (T) *XPC* minigene carrying identical insertions.

exon inclusion (Fig. 3A). In contrast, mutations at positions 3 and 6 led only to a minor decrease of exon skipping, whereas the remaining substitutions had an intermediate effect (Fig. 3A). Of 10 non-C A3 positions, cytosine replacements in at least 6 of them

showed a higher exon inclusion than the remaining nucleotides. These results indicated that AG dinucleotides were core A3 residues that promoted exon repression and that cytosines, which are underrepresented in ESSs (65), were powerful enhancers of exon inclusion in most A3 positions.

Since A_4G_5 and A_9G_{10} were separated by only three nucleotides, their repressive function might be related to interplay between the two closely linked AGs, similar to the effect of neighboring AGs on 3′ ss selection (18, 44). To examine whether the gap between the two AGs affects exon inclusion, we extended the A_4G_5-to-A_9G_{10} distance in the *XPC-T-A3F* minigene from 5 to 7, 9, and 11 nt as shown in Fig. 3B. Constructs extended by 2 and 4 nt resulted in minor increase of exon inclusion levels, whereas further extension eliminated the difference. Thus, extending the AG-AG distance up to 9 nt slightly weakened repressive effect on exon inclusion, although we could not exclude an inhibitory influence of short insertions per se.

Splicing activity of A3 sequences derived from *Alu* subfamilies. *Alu* repeats are composed of J, S, and Y families that are further categorized into subfamilies based on their sequence variability (2, 37). Alignment of *LST1* segment A3 and sequences representative of *Alu* subfamilies (Fig. 3C) showed that nucleotides 1, 6, and 12, which were not essential for exon inclusion (Fig. 3A), were in the most variable positions. To test how natural variability of A3-like *Alu*s affects splicing, we mutated the *XPC-T-A3F* minigene to create constructs that corresponded to consensus sequences of *Alu* subfamilies (Fig. 3C). Interestingly, splicing reporters with variations in positions 9 and 10 showed the greatest reduction of exon skipping, whereas minigenes with mutations in positions 1, 6, and 12 showed no or only minor alterations. A3 segments of *Alu* subfamilies that did not contain A_9G_{10} induced only minor or moderate exon skipping (splicing reporters G, H, J, K, and L in Fig. 3C and D). Thus, A3 derived from FLAM_A, the left arm of *Alu*Jo/Jb/S/Sx/Sq, and the right arm of *Alu*Jo remained strong inhibitors of exon inclusion, whereas segments representing the remaining *Alu* subfamilies were less efficient silencers.

Characterization of *Alu*-derived splicing silencer A2. The importance of two AGs in A3 led us to examine the contribution of four AGs in segment A2 to exon skipping (Fig. 1A and 2A). We analyzed exon skipping in the truncated *XPC* construct, in which segment A2 was inserted in the central exon in the same position as A3. The splicing reporter (termed *XPC-T-A2F*) was mutated in each AG. Figure 4A shows that guanosine-to-cytosine transversions in the first two AGs markedly diminished exon skipping. The same mutation in the fourth AG also reduced exon skipping; however, mutation of the third AG showed little effect.

To compare the influence of A2 segments that were representative of *Alu* subfamilies, we prepared a series of mutated clones B to M (Fig. 4B), transfected them into 293T cells, and examined exon inclusion. Interestingly, exon inclusion levels correlated with the number of intact AGs ($r = 0.66$). Correlation was higher ($r = 0.85$) if minigene J, which contains a mutation in position 15 important for splicing, was disregarded. The presence of three remaining AGs (clones K to M) generated about equal mixtures of exon inclusion and skipping, whereas the presence of only one AG was associated with low
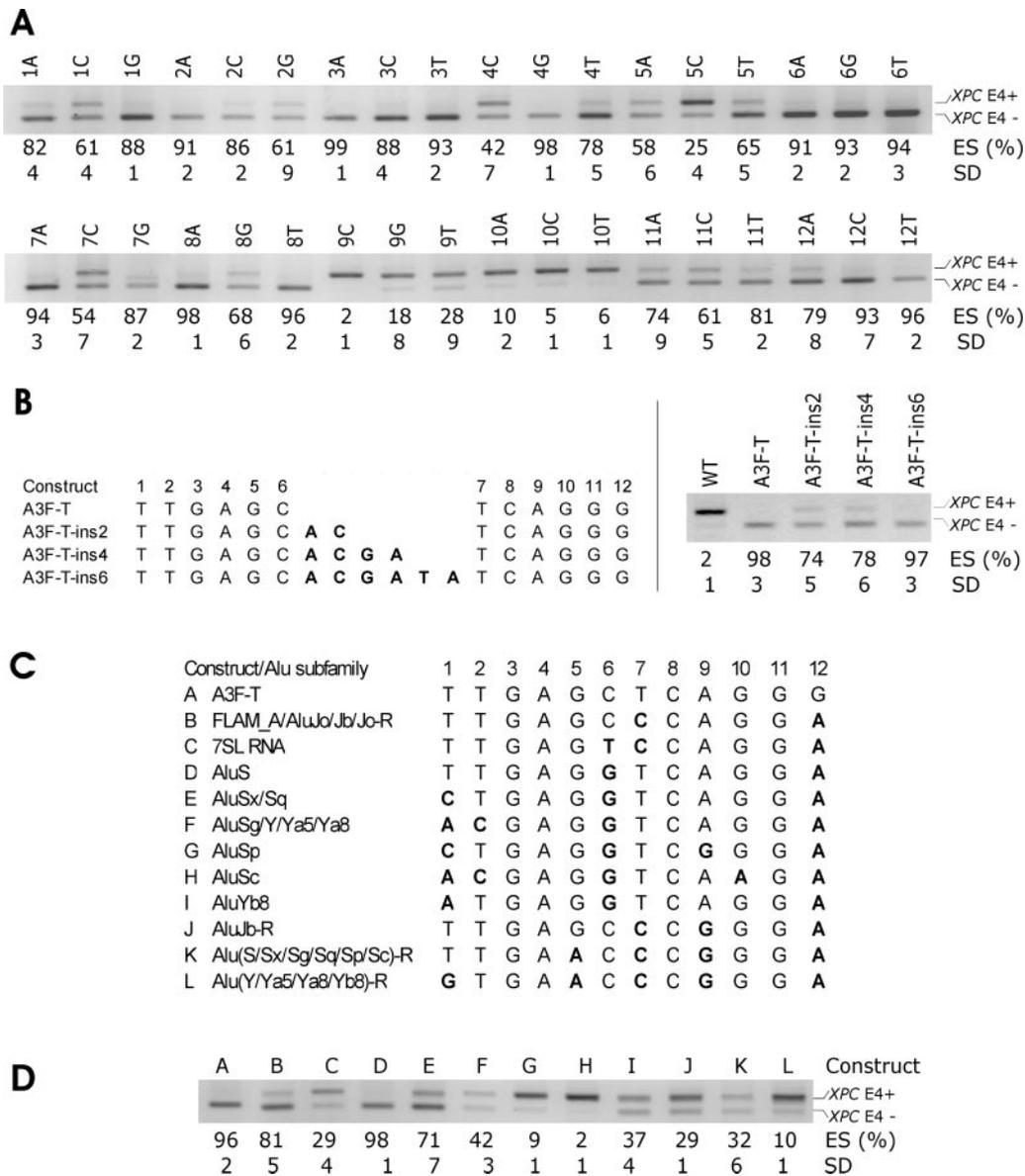
FIG. 3. Characterization of *Alu*-derived splicing silencer A3. (A) Exon inclusion levels following transfection of mutated A3 in *XPC* exon 4. Point mutations above each panel are numbered according to the A3 position as shown in panels B and C. ES, exon skipping as a ratio of transcripts lacking exon 4 (E4−) to the sum of E4− and E4+ transcripts. SD, standard deviation of two transfection experiments. (B) The influence of AG-AG distance in segment A3 on inclusion of a heterologous exon. (Left panel) Two-, 4-, and 6-nt insertions in the *XPC-T-A3F* construct. The *XPC* exon 4 sequences flanking A3 were GTGCTGGGTG (upstream) and ACGTGAGAGA (downstream). (Right panel) Exon inclusion levels from a single transfection experiment in duplicate. (C) Alignment of *LST1* A3 segment and consensus sequences of *Alu* subfamilies. *Alu* sequences were derived from the left arm (2, 37), except for those denoted by -R (the right arm of *Alu*). The designation of *Alu* subfamilies was as described previously (2, 37). Mutations are shown in bold. (D) The influence of minigene mutations in A3 on exon inclusion. Constructs A to L shown at the top correspond to mutations listed in Fig. 3C.

levels of skipping, except for *Alu*Yb8. Constructs containing two AGs (C to E, Fig. 4C) produced intermediate levels. Together, most A2 sequences representative of the left arm of *Alu* showed only a minor increase of exon skipping, whereas those that were characteristic of the right arm were more active.

Identification of a downstream splicing enhancer in sense *Alu*. Comparison of the newly exonized sequences in *LST1*/n with octamer (68)- and RESCUE (23)-derived enhancers revealed a cluster of putative exonic splicing enhancers (designated A4; see Tables S2 and S3 in the supplemental material)

located immediately downstream of segment A3 (Fig. 2A). We deleted the last 16 nt from segment A4 in the *LST1* TNFd-(AG)$_0$ minigene, leaving the first 3 nt in the construct to maintain the flanking sequence of A3 intact. Interestingly, transfection of this minigene into cells transiently expressing ASF/SF2 or SRp40 did not induce *LST1*/n (Fig. 5A), indicating that this element was critical for SR-induced activation of the cryptic 3′ ss. Insertion of A4 in both orientations into exon 12 of the *TH* minigene markedly increased exon inclusion (Fig. 5B), and insertion of both sense and antisense A4 segments into *XPC*

A

	A2F-T	A2R-T	A2F-T-2C	A2F-T-6C	A2F-T-10C	A2F-T-14C	Mutation
							/XPC E4+
							XPC E4-
ES (%)	95	4	3	4	98	42	
SD	2	1	2	1	1	5	

B

	Construct/Alu subfamily	1	2	3	4	5	6	7	8	9	10	11	12	13	14	15	16
A	A2F-T	A	G	G	C	A	G	G	A	A	G	A	T	A	G	C	T
B	7slRNA	A	G	G	C	T	G	G	A	A	G	A	T	C	G	C	T
C	FLAM_A	A	G	G	C	G	G	G	A	G	G	A	T	C	G	C	T
D	AluJo	A	G	G	C	G	G	G	A	G	G	A	T	T	G	C	T
E	AluJb	A	G	G	C	G	G	G	A	G	G	A	T	C	A	C	T
F	AluS	A	G	G	C	G	G	G	C	G	G	A	T	C	A	C	T
G	AluSx/Sp	A	G	G	C	G	G	G	C	G	G	A	T	C	A	C	C
H	AluSg/Sc/Y/Ya5/Ya8	A	G	G	C	G	G	G	C	G	G	A	T	C	A	C	G
I	AluSq	A	G	G	C	G	G	G	T	G	G	A	T	C	A	C	C
J	AluYb8	A	G	G	C	G	G	G	T	G	G	A	T	C	A	T	G
K	Alu(Jo/Jb)-R	A	G	G	C	A	G	G	A	G	G	A	T	C	G	C	T
L	Alu(S/Sx/Sg/Sq/Sc)-R	A	G	G	C	A	G	G	A	G	A	A	T	C	G	C	T
M	Alu(Y/Ya5/Ya8/Yb8)-R	A	G	G	C	A	G	G	A	G	A	A	T	G	G	C	G

C

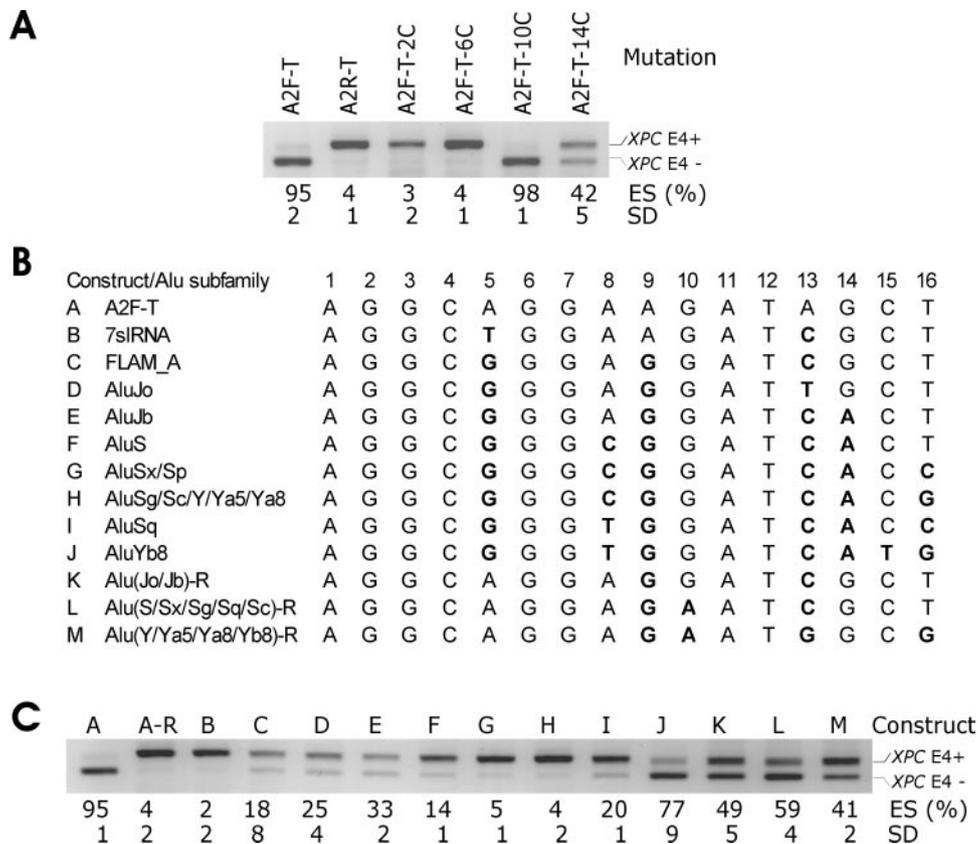|	A	A-R	B	C	D	E	F	G	H	I	J	K	L	M	Construct
															/XPC E4+
															XPC E4-
ES (%)	95	4	2	18	25	33	14	5	4	20	77	49	59	41	
SD	1	2	2	8	4	2	1	1	2	1	9	5	4	2	

FIG. 4. Characterization of splicing silencer A2. (A) The influence of A2 mutations in four AGs on exon inclusion. The splicing reporter constructs are shown at the top. Guanine-to-cytosine mutations are in positions shown in panel B. ES, exon skipping as a ratio of transcripts lacking exon 4 (E4−) to the sum of E4− and E4+ transcripts. SD, standard deviation of two transfection experiments. (B) Alignment of *LST1* segment A2 with consensus sequences of *Alu* subfamilies. Mutations (in bold) that corresponded to sequence variations in the subfamilies were introduced in segment A2 inserted in the *XPC-T* construct in the sense orientation. The designation of *Alu* subfamilies was as described previously (2, 37). (C) Influence of A2 variants representing *Alu* subfamilies on inclusion of *XPC* exon 4 in mRNA. Constructs A to M shown at the top correspond to mutations listed in Fig. 4B. A-R, constructs with segment A2 inserted in the antisense orientation.

exon 4 virtually eliminated exon skipping (data not shown). Since there was no significant difference in exon inclusion between the sense and antisense orientations of A4 in either minigene, we compared the strength of both inserts further in an *XPC* construct with weakened 3′ ss. This construct was created by mutating the *XPC-T* minigene in the BP adenosine that was colocalized previously with a disease-causing mutation in a patient with xeroderma pigmentosum (39). The A→G mutation in predicted BP in the wild-type *XPC-T* minigene increased exon skipping to over 90% (Fig. 5D). Insertion of A4F into the *XPC-T* construct with the BP A→G mutation restored exon 4 inclusion to a level comparable to the wild-type *XPC-T* minigene, whereas A4R showed no effect, indicating that A4F is a stronger splicing enhancer than A4R. Similarly, insertion of A4F into the *TH* minigene carrying an A→G transition of the predicted exon 12 BP (34, 41) rescued splicing (data not shown). Together, these results suggested that A4 contains a splicing enhancer derived from a sense *Alu* that promotes exon inclusion in a heterologous context.

Finally, to determine the extent to which sequence variability in segment A4 in *Alu* subfamilies influences splicing, we transfected the *XPC-T* minigene with the BP A→G transition that was further mutated in A4 as shown in Fig. 5C. In contrast to A4F, which rescued splicing to a level comparable to that of the wild type (Fig. 5D), most A4 sequences derived from other *Alu* subfamilies did not generate significant exon inclusion, with *Alu*Sp-derived A4 exhibiting a moderate effect.

DISCUSSION

We have shown the first examples of splicing silencers and enhancers in sense *Alu* repeats, providing additional evidence for splicing regulatory sequences in these mobile elements, first reported for antisense *Alu*s (22, 60). *Alu*s are primate specific and are present in hundreds of thousands of copies in the human genome, suggesting that splicing silencers identified in this study contribute to repression of a large number of pseudoacceptor sites and that these repeats may provide a substantial reservoir of sequences that inhibit splicing. Since the *Alu*-derived splicing silencers inhibited utilization of a cryptic 3′ ss located in the same repeat, they function to eliminate *Alu* exonization.

Examination of chimeric splicing reporters that contained the newly identified inhibitory sequences highlighted the importance of AG dinucleotides in splice site repression. AGs are commonly found in splicing silencer elements of both mam-
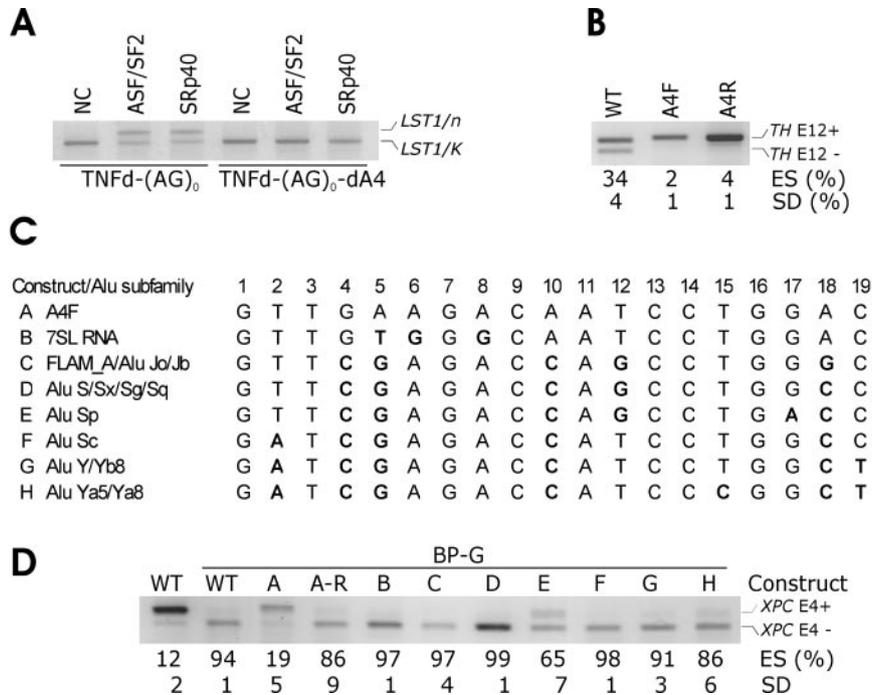
FIG. 5. Identification and characterization of *Alu*-derived splicing enhancer A4. (A) Deletion of A4 in TNFd-(AG)$_0$ constructs eliminated the expression of SRp40- and ASF/SF2-induced *LST1/n*. We used 1 μg of plasmids expressing the two SR proteins and 0.5 μg of the reporter plasmid. NC, no-cotransfection controls. No-template controls are not shown. (B) Insertion of A4 into the *TH* minigene in both sense and antisense orientations resulted in full exon inclusion. The insertions were made in *TH* exon 12. ES, exon skipping as a ratio of transcripts lacking exon 12 (E12−) to the sum of E12− and E12+ transcripts. WT, wild type. SD, standard deviation as calculated from two transfection experiments. (C) Alignment of *LST1* segment A4 with consensus sequences of *Alu* subfamilies. Mutations (in bold) that corresponded to sequence variations in the subfamilies were introduced in segment A4 inserted in the *XPC-T* construct in the sense orientation. The designation of *Alu* subfamilies was as described previously (2, 37). (D) Splicing of the *XPC-T* minigene containing the branchpoint A→G mutation could be rescued by A4F but not by A4 sequences representing most *Alu* subfamilies. BP-G, constructs containing the adenine-to-guanine mutation in the predicted branchpoint of *XPC* exon 4. Constructs A to H shown at the top correspond to mutations listed in panel C. A-R, construct with segment A4 inserted in the antisense orientation.

malian (17, 21, 26, 38, 49) and viral (4, 54, 59, 62, 70) pre-mRNAs and are also common in groups B and D to G of ESSs that have been recently identified through comprehensive fluorescence-activated screens (FAS) (65). Although they were neither over- nor underrepresented among FAS ESSs (65), only 16 of 85 (18.8%) informative AGs found in 133 nonrepetitive FAS ESS decamers were preceded by a purine, whereas the majority of the remaining AGs had uracil in this position (67/69; 97.1%). Similarly, only three of 79 (3.8%) informative FAS ESS AGs were preceded by purine dinucleotides, whereas 38/79 (48.1%) FAS ESS AGs were preceded by pyrimidine dinucleotides ($P < 10^{-4}$, assuming independence).

The occurrence of nucleotides that precede AGs in FAS ESSs ($T_{67} > A_{13} > G_3 > C_2$) is similar to a C>T>A>G hierarchy observed for the vertebrate 3′ ss (48, 56, 67), except for a depletion of cytosines in this position among FAS ESSs. The efficiency of CAG 3′ ss in in vitro splicing reactions was comparable to that of UAGs (56), raising speculation that a higher proportion of cytosines versus uracils in position −3 of authentic 3′ ss might be linked to a silencer effect of UAG pseudoacceptors. In addition to FAS ESS, UAGs predominate also in other ESSs (4, 21, 36, 38, 54, 59, 66), although winner decamers identified by selection experiments contained cytosines in this position (22). Similarly, our inspection of previously identified ESSs (reviewed in reference 69) showed that AGs preceded by

dipurines were extremely rare, whereas RRAGs dominated purine-rich ESEs. This is consistent with the observed lack of efficient exonization in our splicing reporter mutated in the third AG of A2, which was preceded by two purines (Fig. 4A). In addition, A3 mutations 3T and 8T that introduced uracils in front of the critical AG dinucleotides were associated with almost full exon skipping, whereas an A3 2G mutation, which creates a dipurine in front of the same AG, increased exon inclusion (Fig. 3A).

The importance of AGs in repression of 3′ ss selection is also supported by rare cases of disease-causing splicing mutations that create new AGs between BPS and authentic 3′ AG. Although they usually create de novo acceptor sites, as first described for *HBB* (11), at least several well-documented reports (7, 8, 24, 29) showed that these AGs suppressed authentic acceptor sites, while activating a cryptic 3′ ss further upstream of the BPS (I. Vořechovský et al., in preparation).

Together, the above observations suggest that AGs represent important motifs in the RNA splicing code that governs 3′ ss selection. As for the splice-like sequences proposed to negatively regulate authentic 5′ ss (15, 21, 22, 55, 60, 65), inhibitory pseudoacceptors identified in this study may act in a similar manner, most likely by recruiting components of the spliceosome to inappropriate places where they compete for interactions with genuine 3′ ss. These signals are likely to be

partially recognized by splicing factors such as U2 snRNP (36), but may not assemble fully functional splicing complexes (50). The results of our initial experiment, in which the A_4G_5-A_9G_{10} distance was modified in segment A3 (Fig. 3B), were not inconsistent with the notion that complexes assembled at the authentic 3′ ss and A3 AGs share common spliceosomal components and similar AG-AG measuring mechanisms.

Segment A3 (Fig. 2B and 3B) contains an AGGG motif that was previously shown to interact with several *trans*-acting factors, including hnRNP A1 (9) and the H family of hnRNPs (5, 14). Interestingly, our inspection of FAS ESS sequences showed that guanosine was the most frequent nucleotide in a position that immediately followed FAS ESS AGs, whereas cytosines and adenines were underrepresented ($G_{44}>T_{33}>A_2>C_1$). In addition, all AGs in FAS ESS decamers that were obtained twice in independent transfections were followed by guanine. GG dinucleotides were also overrepresented in two positions that followed FAS ESS AGs (14 among 74 AGs, versus the ~5 expected; $P < 0.001$). However, the AGGG motif alone did not appear to explain all the observed effects, since the A-to-G mutation in position 6 of A1 (Fig. 2A), which creates an AGGG signature, increased exon skipping only from ~12 to ~30% (data not shown). Our systematic mutagenesis showed (Fig. 3A) that AG dinucleotides in this motif were critical, whereas the second and third guanines in the G triplet were less important for exon repression. Thus, future studies should determine if these *trans*-acting factors differentially interact with RNAs transcribed from our mutated constructs.

The apparent lack of *LST1/n* in the wild-type construct (Fig. 1B) could be due to a silencing effect of TNFd on cryptic 3′ ss activation or impaired amplification and/or reverse transcription of repeat-containing transcripts. To address the latter hypothesis, we examined the amplification yield of plasmids with and without TNFd. The yield of PCR products was slightly lower for TNFd-containing plasmids than for those lacking the repeat (43). However, separate transcription of the two plasmids in vitro and repeated treatment with DNase I followed by RT-PCR of mixed cDNAs showed a substantial decrease of signal intensity from TNFd-containing transcript, indicating that the detection bias toward templates lacking TNFd was introduced mainly by the RT step (43; data not shown). The insertion of TNFd into a PY7 construct, which is spliced efficiently in vitro (20), did not reduce in vitro splicing as compared to the wild-type PY7 in 30- to 90-min reactions (43; data not shown). However, this construct has a very strong PPT (20), which is a central splicing recognition element of human introns, and a putative weak silencing effect of TNFd may not be revealed. Thus, rigorous evidence for a direct TNFd role in splicing inhibition will require further studies. TNFd is not a perfect AG repeat since it has two AGGG tetramers both in the middle and at the 3′ end (see Fig. S1 in the supplemental material) that may recruit *trans*-acting factors that directly contact A3 in the pre-mRNA or may prevent accessibility of the cryptic 3′ ss through secondary structure.

Finally, antisense *Alu*s are amenable to exonization as they contain a strong PPT and many potential 3′ and 5′ ss, whereas exonization of sense *Alu*s is less common due to a lack of strong PPT and a lower number of both 3′ and 5′ ss (44, 57, 58). Since antisense *Alu*s contain sequences that inhibit (22, 60) and enhance (H. Lei, I. Day, and I. Vořechovský, submitted for publication) *Alu* inclusion in mature transcripts, *Alu*-derived

silencers identified in this study may contribute to a low exonization potential of sense *Alu*s. It will be interesting to test this hypothesis in future studies by modifying splicing consensus signals of naturally occurring sense *Alu*s in human introns.

REFERENCES

1. **Arrisi-Mercado, P., M. Romano, A. F. Muro, and F. E. Baralle.** 2004. An exonic splicing enhancer offsets the atypical GU-rich 3′ splice site of human apolipoprotein A-II exon 3. J. Biol. Chem. **279:**39331–39339.
2. **Batzer, M. A., and P. L. Deininger.** 2002. Alu repeats and human genomic diversity. Nat. Rev. Genet. **3:**370–379.
3. **Berget, S. M.** 1995. Exon recognition in vertebrate splicing. J. Biol. Chem. **270:**2411–2414.
4. **Bilodeau, P. S., J. K. Domsic, A. Mayeda, A. R. Krainer, and C. M. Stoltzfus.** 2001. RNA splicing at human immunodeficiency virus type 1 3′ splice site A2 is regulated by binding of hnRNP A/B proteins to an exonic splicing silencer element. J. Virol. **75:**8487–8497.
5. **Blanchette, M., and B. Chabot.** 1999. Modulation of exon skipping by high-affinity hnRNP A1-binding sites and by intron elements that repress splice site utilization. EMBO J. **18:**1939–1952.
6. **Blencowe, B. J.** 2000. Exonic splicing enhancers: mechanism of action, diversity and role in human genetic diseases. Trends Biochem. Sci. **25:**106–110.
7. **Brand, K., K. A. Dugi, J. D. Brunzell, D. N. Nevin, and S. Santamarina-Fojo.** 1996. A novel A→G mutation in intron I of the hepatic lipase gene leads to alternative splicing resulting in enzyme deficiency. J. Lipid Res. **37:**1213–1223.
8. **Bruggenwirth, H. T., A. L. Boehmer, S. Ramnarain, M. C. Verleun-Mooijman, D. P. Satijn, J. Trapman, J. A. Grootegoed, and A. O. Brinkmann.** 1997. Molecular analysis of the androgen-receptor gene in a family with receptor-positive partial androgen insensitivity: an unusual type of intronic mutation. Am. J. Hum. Genet. **61:**1067–1077.
9. **Burd, C. G., and G. Dreyfuss.** 1994. RNA binding specificity of hnRNP A1: significance of hnRNP A1 high-affinity binding sites in pre-mRNA splicing. EMBO J. **13:**1197–1204.
10. **Burge, C. B., T. Tuschl, and P. A. Sharp.** 1999. Splicing of precursors to mRNAs by the spliceosome, p. 525–560. *In* R. F. Gesteland, T. R. Cech, and J. F. Atkins (ed.), The RNA world. Cold Spring Harbor Laboratory Press, New York, N.Y.
11. **Busslinger, M., N. Moschonas, and R. A. Flavell.** 1981. Beta$^+$ thalassemia: aberrant splicing results from a single point mutation in an intron. Cell **27:**289–298.
12. **Cáceres, J. F., T. Misteli, G. R. Screaton, D. L. Spector, and A. R. Krainer.** 1997. Role of the modular domains of SR proteins in subnuclear localization and alternative splicing specificity. J. Cell Biol. **138:**225–238.
13. **Cáceres, J. F., G. R. Screaton, and A. R. Krainer.** 1998. A specific subset of SR proteins shuttles continuously between the nucleus and the cytoplasm. Genes Dev. **12:**55–66.
14. **Caputi, M., and A. M. Zahler.** 2001. Determination of the RNA binding specificity of the heterogeneous nuclear ribonucleoprotein (hnRNP) H/H′/F/2H9 family. J. Biol. Chem. **276:**43850–43859.
15. **Carothers, A. M., G. Urlaub, D. Grunberger, and L. A. Chasin.** 1993. Splicing mutants and their second-site suppressors at the dihydrofolate reductase locus in Chinese hamster ovary cells. Mol. Cell. Biol. **13:**5085–5098.
16. **Cartegni, L., S. L. Chew, and A. R. Krainer.** 2002. Listening to silence and understanding nonsense: exonic mutations that affect splicing. Nat. Rev. Genet. **3:**285–298.
17. **Chew, S. L., L. Baginsky, and I. C. Eperon.** 2000. An exonic splicing silencer in the testes-specific DNA ligase III beta exon. Nucleic Acids Res. **28:**402–410.
18. **Chua, K., and R. Reed.** 2001. An upstream AG determines whether a downstream AG is selected during catalytic step II of splicing. Mol. Cell. Biol. **21:**1509–1514.
19. **de Baey, A., B. Fellerhoff, S. Maier, S. Martinozzi, U. Weidle, and E. H. Weiss.** 1997. Complex expression pattern of the TNF region gene LST1 through differential regulation, initiation, and alternative splicing. Genomics **45:**591–600.
20. **Deirdre, A., J. Scadden, and C. W. Smith.** 1995. Interactions between the

terminal bases of mammalian introns are retained in inosine-containing pre-mRNAs. EMBO J. **14:**3236–3246.

21. **Del Gatto, F., and R. Breathnach.** 1995. Exon and intron sequences, respectively, repress and activate splicing of a fibroblast growth factor receptor 2 alternative exon. Mol. Cell. Biol. **15:**4825–4834.

22. **Fairbrother, W. G., and L. A. Chasin.** 2000. Human genomic sequences that inhibit splicing. Mol. Cell. Biol. **20:**6816–6825.

23. **Fairbrother, W. G., R. F. Yeh, P. A. Sharp, and C. B. Burge.** 2002. Predictive identification of exonic splicing enhancers in human genes. Science **297:**1007–1013.

24. **Fujimaru, M., A. Tanaka, K. Choeh, N. Wakamatsu, H. Sakuraba, and G. Isshiki.** 1998. Two mutations remote from an exon/intron junction in the beta-hexosaminidase beta-subunit gene affect 3′-splice site selection and cause Sandhoff disease. Hum. Genet. **103:**462–469.

25. **Gabellini, N.** 2001. A polymorphic GT repeat from the human cardiac Na+Ca2+ exchanger intron 2 activates splicing. Eur. J. Biochem. **268:**1076–1083.

26. **Graham, I. R., M. Hamshere, and I. C. Eperon.** 1992. Alternative splicing of a human α-tropomyosin muscle-specific exon: identification of determining sequences. Mol. Cell. Biol. **12:**3872–3882.

27. **Graveley, B. R., K. J. Hertel, and T. Maniatis.** 1999. SR proteins are 'locators' of the RNA splicing machinery. Curr. Biol. **9:**R6–R7.

28. **Hefferon, T. W., J. D. Groman, C. E. Yurk, and G. R. Cutting.** 2004. A variable dinucleotide repeat in the CFTR gene contributes to phenotype diversity by forming RNA secondary structures that alter splicing. Proc. Natl. Acad. Sci. USA **101:**3504–3509.

29. **Higashi, Y., A. Tanae, H. Inoue, T. Hiromasa, and Y. Fujii-Kuriyama.** 1988. Aberrant splicing and missense mutations cause steroid 21-hydroxylase [P-450(C21)] deficiency in humans: possible gene conversion products. Proc. Natl. Acad. Sci. USA **85:**7486–7490.

30. **Ho, S. N., H. D. Hunt, R. M. Horton, J. K. Pullen, and L. R. Pease.** 1989. Site-directed mutagenesis by overlap extension using the polymerase chain reaction. Gene **77:**51–59.

31. **Holzinger, I., A. de Baey, G. Messer, G. Kick, H. Zwierzina, and E. H. Weiss.** 1995. Cloning and genomic characterization of *LST1*: a new gene in the human TNF region. Immunogenetics **42:**315–322.

32. **Howe, K. J., and M. Ares, Jr.** 1997. Intron self-complementarity enforces exon inclusion in a yeast pre-mRNA. Proc. Natl. Acad. Sci. USA **94:**12467–12472.

33. **Hui, J., K. Stangl, W. S. Lane, and A. Bindereif.** 2003. HnRNP L stimulates splicing of the eNOS gene by binding to variable-length CA repeats. Nat. Struct. Biol. **10:**33–37.

34. **Janssen, R. J., R. A. Wevers, M. Haussler, J. A. Luyten, G. C. Steenbergen-Spanjers, G. F. Hoffmann, T. Nagatsu, and L. P. Van den Heuvel.** 2000. A branch site mutation leading to aberrant splicing of the human tyrosine hydroxylase gene in a child with a severe extrapyramidal movement disorder. Ann. Hum. Genet. **64:**375–382.

35. **Jurka, J., and E. Zuckerkandl.** 1991. Free left arms as precursor molecules in the evolution of Alu sequences. J. Mol. Evol. **33:**49–56.

36. **Kan, Z., and M. R. Green.** 1999. Pre-mRNA splicing of IgM exons M1 and M2 is directed by a juxtaposed splicing enhancer and inhibitor. Genes Dev. **13:**462–471.

37. **Kapitonov, V., and J. Jurka.** 1996. The age of Alu subfamilies. J. Mol. Evol. **42:**59–65.

38. **Kashima, T., and J. L. Manley.** 2003. A negative element in SMN2 exon 7 inhibits splicing in spinal muscular atrophy. Nat. Genet. **34:**460–463.

39. **Khan, S. G., A. Metin, E. Gozukara, H. Inui, T. Shahlavi, V. Muniz-Medina, C. C. Baker, T. Ueda, J. R. Aiken, T. D. Schneider, and K. H. Kraemer.** 2003. Two essential splice lariat branchpoint sequences in one intron in a xeroderma pigmentosum DNA repair gene: mutations result in reduced XPC mRNA levels that correlate with cancer risk. Hum. Mol. Genet. **13:**343–352.

40. **Krainer, A. R., G. C. Conway, and D. Kozak.** 1990. The essential pre-mRNA splicing factor SF2 influences 5′ splice site selection by activating proximal sites. Cell **62:**35–42.

41. **Královičová, J., S. Houngninou-Molango, A. Krämer, and I. Vořechovský.** 2004. Branch sites haplotypes that control alternative splicing. Hum. Mol. Genet. **13:**3189–3202.

42. **Lehner, B., J. I. Semple, S. E. Brown, D. Counsell, R. D. Campbell, and C. M. Sanderson.** 2004. Analysis of a high-throughput yeast two-hybrid system and its use to predict the function of intracellular proteins encoded within the human MHC class III region. Genomics **83:**153–167.

43. **Lei, H.** 2004. Ph.D. thesis. Karolinska Institute, Stockholm, Sweden.

44. **Lev-Maor, G., R. Sorek, N. Shomron, and G. Ast.** 2003. The birth of an alternatively spliced exon: 3′ splice-site selection in Alu exons. Science **300:**1288–1291.

45. **Makalowski, W.** 2003. Genomics. Not junk after all. Science **300:**1246–1247.

46. **Makalowski, W., G. A. Mitchell, and D. Labuda.** 1994. Alu sequences in the coding regions of mRNA: a source of protein variability. Trends Genet. **10:**188–193.

47. **Mitchell, G. A., D. Labuda, G. Fontaine, J. M. Saudubray, J. P. Bonnefont, S. Lyonnet, L. C. Brody, G. Steel, C. Obie, and D. Valle.** 1991. Splice-mediated insertion of an Alu sequence inactivates ornithine delta-aminotransferase: a role for Alu elements in human mutation. Proc. Natl. Acad. Sci. USA **88:**815–819.

48. **Mount, S. M.** 1982. A catalogue of splice junction sequences. Nucleic Acids Res. **10:**459–472.

49. **Muro, A. F., M. Caputi, R. Pariyarath, F. Pagani, E. Buratti, and F. E. Baralle.** 1999. Regulation of fibronectin EDA exon alternative splicing: possible role of RNA secondary structure for enhancer display. Mol. Cell. Biol. **19:**2657–2671.

50. **Nemeroff, M. E., U. Utans, A. Krämer, and R. M. Krug.** 1992. Identification of *cis*-acting intron and exon regions in influenza virus NS1 mRNA that inhibit splicing and cause the formation of aberrantly sedimenting presplicing complexes. Mol. Cell. Biol. **12:**962–970.

51. **Niksic, M., M. Romano, E. Buratti, F. Pagani, and F. E. Baralle.** 1999. Functional analysis of cis-acting elements regulating the alternative splicing of human CFTR exon 9. Hum. Mol. Genet. **8:**2339–2349.

52. **Raghunathan, A., R. Sivakamasundari, J. Wolenski, R. Poddar, and S. M. Weissman.** 2001. Functional analysis of B144/LST1: a gene in the tumor necrosis factor cluster that induces formation of long filopodia in eukaryotic cells. Exp. Cell Res. **268:**230–244.

53. **Rollinger-Holzinger, I., B. Eibl, M. Pauly, U. Griesser, F. Hentges, B. Auer, G. Pall, P. Schratzberger, D. Niederwieser, E. H. Weiss, and H. Zwierzina.** 2000. LST1: a gene with extensive alternative splicing and immunomodulatory function. J. Immunol. **164:**3169–3176.

54. **Si, Z., B. A. Amendt, and C. M. Stoltzfus.** 1997. Splicing efficiency of human immunodeficiency virus type 1 tat RNA is determined by both a suboptimal 3′ splice site and a 10 nucleotide exon splicing silencer element located within tat exon 2. Nucleic Acids Res. **25:**861–867.

55. **Siebel, C. W., L. D. Fresco, and D. C. Rio.** 1992. The mechanism of somatic inhibition of Drosophila P-element pre-mRNA splicing: multiprotein complexes at an exon pseudo-5′ splice site control U1 snRNP binding. Genes Dev. **6:**1386–1401.

56. **Smith, C. W. J., T. T. Chu, and B. Nadal-Ginard.** 1993. Scanning and competition between AGs are involved in 3′ splice site selection in mammalian introns. Mol. Cell. Biol. **13:**4939–4952.

57. **Sorek, R., G. Ast, and D. Graur.** 2002. Alu-containing exons are alternatively spliced. Genome Res. **12:**1060–1067.

58. **Sorek, R., G. Lev-Maor, M. Reznik, T. Dagan, F. Belinky, D. Graur, and G. Ast.** 2004. Minimal conditions for exonization of intronic sequences: 5′ splice site formation in *Alu* exons. Mol. Cell **14:**221–231.

59. **Staffa, A., and A. Cochrane.** 1995. Identification of positive and negative splicing regulatory elements within the terminal *tat-rev* exon of human immunodeficiency virus type 1. Mol. Cell. Biol. **15:**4597–4605.

60. **Sun, H., and L. A. Chasin.** 2000. Multiple splicing defects in an intronic false exon. Mol. Cell. Biol. **20:**6414–6425.

61. **Tacke, R., and J. L. Manley.** 1999. Determinants of SR protein specificity. Curr. Opin. Cell Biol. **11:**358–362.

62. **Tomonaga, K., T. Kobayashi, B. J. Lee, M. Watanabe, W. Kamitani, and K. Ikuta.** 2000. Identification of alternative splicing and negative splicing activity of a nonsegmented negative-strand RNA virus, Borna disease virus. Proc. Natl. Acad. Sci. USA **97:**12788–12793.

63. **Udalova, I. A., S. A. Nedospasov, G. C. Webb, D. D. Chaplin, and R. L. Turetskaya.** 1993. Highly informative typing of the human TNF locus using six adjacent polymorphic markers. Genomics **16:**180–186.

64. **Vořechovský, I., L. Luo, M. J. Dyer, D. Catovsky, P. L. Amlot, J. C. Yaxley, L. Foroni, L. Hammarstrom, A. D. Webster, and M. A. Yuille.** 1997. Clustering of missense mutations in the ataxia-telangiectasia gene in a sporadic T-cell leukaemia. Nat. Genet. **17:**96–99.

65. **Wang, Z., M. E. Rolish, G. Yeo, V. Tung, M. Mawson, and C. B. Burge.** 2004. Systematic identification and analysis of exonic splicing silencers. Cell **119:**831–845.

66. **Wentz, M. P., B. E. Moore, M. W. Cloyd, S. M. Berget, and L. A. Donehower.** 1997. A naturally arising mutation of a potential silencer of exon splicing in human immunodeficiency virus type 1 induces dominant aberrant splicing and arrests virus production. J. Virol. **71:**8542–8551.

67. **Yeo, G., S. Hoon, B. Venkatesh, and C. B. Burge.** 2004. Variation in sequence and organization of splicing regulatory elements in vertebrate genes. Proc. Natl. Acad. Sci. USA **101:**15000–15005.

68. **Zhang, X. H., and L. A. Chasin.** 2004. Computational definition of sequence motifs governing constitutive exon splicing. Genes Dev. **18:**1241–1250.

69. **Zheng, Z. M.** 2004. Regulation of alternative RNA splicing by exon definition and exon sequences in viral and mammalian gene expression. J. Biomed. Sci. **11:**278–294.

70. **Zheng, Z. M., M. Huynen, and C. C. Baker.** 1998. A pyrimidine-rich exonic splicing suppressor binds multiple RNA splicing factors and inhibits spliceosome assembly. Proc. Natl. Acad. Sci. USA **95:**14088–14093.